combination bands or overtones can be ruled out on the basis of symmetry.

Conclusion

The spectrum of $C_2H_7^+$ has been presented. The spectrum shows a strong dependence both on the ratio of ethane to hydrogen and on the backing pressure used. Evidence has been presented in support of our belief that the different behavior can be attributed to the changing ratio of classical to bridged protonated ethane

being probed spectroscopically. The observed infrared frequencies are compared with predicted frequencies for the classical and bridged structures.

Spectral Evidence of Spontaneous Racemic and "Pseudoracemic" Interactions between Optically Active Poly(pyridyl) Metal Chelates Adsorbed on Smectite Clays

Vishwas Joshi and Pushpito K. Ghosh*

Contribution from the Alchemie Research Centre, Thane Belapur Road, Thane-400601, Maharashtra, India. Received September 26, 1988

Abstract: UV–visible absorption and emission spectral studies are reported for enantiomeric (Δ-$(-)_D$, Λ-$(+)_D$) and racemic (Δ,Λ) $Ru(bpy)_3^{2+}$ (bpy = 2,2'-bipyridine) adsorbed on three naturally occurring smectite clays. The results highlight differences in the binding modes of the two forms at low (1–4%) loading levels. The effects of optical purity, loading level, mode of addition of complex, and clay type are also discussed. The observed differences in binding state are ascribed to spontaneous interactions between optical antipodes (racemic interactions). The quenching effect of coadsorbed Δ,Λ-$Co(phen)_3^{2+/3+}$, Λ-$(+)_D$-$Ni(phen)_3^{2+}$, and Λ-$(+)_D$-$Rh(phen)_3^{3+}$ (phen = 1,10-phenanthroline) on the luminescence of Δ-$(-)_D$-, Λ-$(+)_D$-, and Δ,Λ-$Ru(bpy)_3^{2+*}$ is also described. The Stern–Volmer data are rationalized in terms of differences in electron/energy transfer quenching efficiencies between homochiral and heterochiral systems, and luminescence variations arising from binding-state perturbations due to "pseudoracemic" interactions. Such an interpretation is supported by studies with Δ,Λ-$Zn(phen)_3^{2+}$, a structurally analogous, "nonquenching" coadsorbate. Finally, the possible factors that might enhance chiral recognition within clay are discussed.

Optically active poly(pyridyl) chelates of a range of transition-metal ions exhibit a high degree of stereospecificity in binding to DNA[1] and expandable layer lattice (smectite) clays.[2] However, the stereospecificity encountered with the latter is unique in the sense that the clays, being achiral, do not discriminate between enantiomers as such but promote their mutual recognition. This remarkable phenomenon—first reported by Yamagishi[2b]—has led to the development of versatile clay-based systems for optical resolution of racemates[2a,3,4] and for asymmetric synthesis.[5] Recognition between optical antipodes of chelates containing dissimilar metals, e.g., $Ru(phen)_3^{2+}$ and $Co(phen)_3^{2+}$, might also have some bearing on the design of clay-supported bimetallic catalysts from ion-exchanged chiral precursor complexes.[6] The study of clay–chiral molecule interactions is of some fundamental interest as well, since clays might have played an important role in the chiral enrichment process during prebiotic evolution and in the subsequent synthesis of more complex molecular forms.[7,8]

Yamagishi has proposed that poly(pyridyl) metal complexes intercalate in clay as racemic pairs and that this cooperativity for racemic adsorption arises from the rigorous steric requirements essential for closest packing over the clay surface.[2a,c] On the other hand, X-ray powder diffraction studies on Δ,Λ-$Fe(phen)_3^{2+}$–hectorite[9] and time-resolved luminescence studies on Δ,Λ-$Ru(bpy)_3^{2+*}$–hectorite as a function of excitation intensity[10a] have shown that these metal chelates aggregate within the clay matrix even at loading levels as lows as 2% of the cation-exchange capacity. It appeared to us that the twin phenomena of aggregation and racemic pairing may both arise as a consequence of spontaneous interactions between optical antipodes. Preliminary absorption and emission spectral studies on smectite clays lightly loaded with enantiomeric and racemic poly(pyridyl)–Ru(II) chelates have provided strong evidence in support of this hypothesis.[11] In continuation of the above work we report here detailed spectral studies on Δ-$(-)_D$-, Λ-$(+)_D$-, and Δ,Λ-$Ru(bpy)_3^{2+}$ adsorbed on three naturally occurring smectite clays and contrast these findings with those of the complex adsorbed on micellar

(1) (a) Barton, J. K. *Science* **1986**, *233*, 727, and references therein. (b) Yamagishi, A. *J. Phys. Chem.* **1981**, *88*, 5709.

(2) (a) Yamagishi, A. *J. Coord. Chem.* **1987**, *6*, 131. (b) Yamagishi, A.; Soma, M. *J. Am. Chem. Soc.* **1981**, *103*, 4640. (c) Yamagishi, A. *J. Phys. Chem.* **1982**, *86*, 2472. (d) Yamagishi, A.; Fujita, N. *J. Colloid. Interface Sci.* **1984**, *100*, 1778. (e) Turro, N. J.; Kumar, C. V.; Grauer, Z.; Barton, J. K. *Langmuir* **1987**, *3*, 1056, and references therein.

(3) Yamagishi, A. *J. Am. Chem. Soc.* **1985**, *107*, 732.

(4) Kotkar, D.; Ghosh, P. K. *Inorg. Chem.* **1987**, *26*, 208.

(5) (a) Yamagishi, A. *J. Chem. Soc., Chem. Commun.* **1986**, 290. (b) Yamagishi, A.; Aramata, A. *J. Chem. Soc., Chem. Commun.* **1984**, 452.

(6) Efficient hydrogenation catalysts can be obtained from clays exchanged with poly(pyridyl) Ru and Rh chelates, through calcination and subsequent activation under hydrogen (Kotkar, D.; Joshi, V.; Ghosh, P. K., unpublished results).

(7) (a) Tsvetkov, F.; Mingelgrin, V. *Clays Clay Miner.* **1987**, *35*, 391, and references therein.

(8) (a) Cairns-Smith, A. G. *Sci. Am.* **1985**, *252*, 74. (b) Bernal, J. D. *The Origin of Life*; Weidenfeld & Nicholson: London, 1967; p 57. (c) Ponnamperuma, C.; Shimoyamaad, A.; Friebele, E. *Origins Life* **1982**, *12*, 9. (d) Weiss, A. *Angew. Chem., Int. Ed. Engl.* **1981**, *20*, 850.

(9) Berkheiser, V. E.; Mortland, M. M. *Clays Clay Miner.* **1977**, *25*, 105.

(10) (a) Ghosh, P. K.; Bard, A. J. *J. Phys. Chem.* **1984**, *88*, 5519. (b) Similar aggregation effects have also been reported for an anionic Ru(II) chelate intercalated in synthetic hydrotalcite clays. (Giannelis, E. P.; Nocera, D. G.; Pinnavaia, T. J. *Inorg. Chem.* **1987**, *26*, 203). (c) Aggregation effects are not unique to poly(pyridyl) metal chelates. Aggregation of organometallic complex "pillars" on synthetic fluorhectorite and montmorillonite has also been reported (Tsvetkov, F.; White, J. *J. Am. Chem. Soc.* **1988**, *110*, 3183).

(11) (a) Joshi, V.; Kotkar, D.; Ghosh, P. K. *J. Am. Chem. Soc.* **1986**, *108*, 4650. (b) Joshi, V.; Ghosh, P. K. *J. Chem. Soc., Chem. Commun.* **1987**, 789.

Poly(pyridyl) Metal Chelates

J. Am. Chem. Soc., Vol. 111, No. 15, 1989 5605

sodium dodecyl sulfate (SDS) and the perfluorinated cation-exchange polymer Nafion (Du Pont). We have also investigated the effect of coadsorbed Δ,Λ-Zn(phen)$_3$$^{2+}$, Δ,Λ-Co(phen)$_3$$^{2+/3+}$, Λ-(+)$_D$-Ni(phen)$_3$$^{2+}$, and Λ-(+)$_D$-Rh(phen)$_3$$^{3+}$ on the absorption and emission properties of the Ru(II) chelates and have obtained direct evidence of spontaneous "pseudoracemic" interactions. Ru(bpy)$_3$$^{2+}$ was chosen as the probe for this study because of its stability, ease of resolution, inertness to racemization,[12] pronounced spectral features, prior knowledge of its ground- and excited-state properties,[13] and previous literature data on its intercalation.[2e,10a,14-16]

Experimental Section

Materials. The smectite clays used in this work are hectorite from San Bernadino County, CA (SHCa-1, Clay Minerals Repository, University of Missouri), low-iron montmorillonite from Wyoming bentonite (GK 129, Georgia Kaolin Co.), and montmorillonite from Gujarat (VeeClay WE, Cutch Oil and Allied Ind. Ltd., India). The clays were converted into the Na$^+$-exchanged form through mechanical stirring in 1 M NaCl (60 mL/g of clay) for 3 days, followed by purification via repetitive high-speed (15000 rpm) centrifugation and redispersion of residue in triply distilled water (six times). The colloidal dispersion was finally centrifuged at 7000 rpm to separate heavier particles and subsequently dialyzed for 3 days with intermittent replacement of water. The clay concentration was typically 10–12 g/L at the end of dialysis. The stock solution of clay was further diluted with triply distilled water and sonicated prior to use. The cation-exchange capacities (cec) of the dispersed clays were estimated through ion exchange of a known weight of clay with excess Λ-(+)$_D$-Ru(bpy)$_3$$^{2+}$. The flocculated clays were then centrifuged, washed with water, and recentrifuged to remove any superficially adsorbed Ru(II). The amount of chelate adsorbed was determined spectrophotometrically by measuring the absorbances of the initial and final solutions. The cec values were 1.02, 0.94, and 1.04 mequiv/g for SHCa-1, GK 129, and Vee Clay WE, respectively, in good agreement with the reported values for such clay types.[14,15]

Δ,Λ-Ru(bpy)$_3$Cl$_2$ was synthesized by the method of Braddock and Meyer[17] and recrystallized from hot water. Elemental analysis of the corresponding perchlorate salt was in satisfactory agreement with the formula Ru(bpy)$_3$(ClO$_4$)$_2$ (obsd N = 10.70%, C = 46.47%, H = 3.11%; calcd N = 10.93%, C = 46.87%, H = 3.12%). Optical resolution of the above complex was achieved by a modification of the procedure of Dwyer and Gyarfas.[18] The process involved mixing of an aqueous solution of Δ,Λ-Ru(bpy)$_3$Cl$_2$·6H$_2$O (5.96 mmol in 80 mL) with a solution containing 7.90 mmol of potassium antimonyl tartrate (K(+)-SbO·Tart) and 4.0 mmol of potassium iodide in 80 mL of water. The mixture was left standing for 30 min and subsequently filtered on a sintered funnel. The residue [Δ-(-)$_D$-Ru(bpy)$_3$·((+)-SbO·Tart)$_2$]$_2$·Δ-(-)$_D$-Ru(bpy)$_3$I$_2$·18H$_2$O[18] was washed, and the washings were discarded. A saturated KBr solution (5 mL) was added to the filtrate, whereupon red crystals of Λ-(+)$_D$-Ru(bpy)$_3$Br$_2$ were formed.[19] The Δ-(-)$_D$ enantiomer was obtained by redissolving the initial residue in 50 mL of a hot (70–80 °C) solution of 0.05 M NaOH, filtering the solution, and adding saturated KBr (5 mL) to precipitate the complex. The bromide salts were recrystallized from hot water until constant optical rotation values were obtained (four recrystallizations generally sufficed) and subsequently converted into the perchlorate salts. The analytical data [Δ-(-)$_D$: N = 10.47%, C = 44.88%, H = 3.20%; Λ-(+)$_D$: N = 10.56%, C = 45.45%, H = 3.25%] were in agreement with the formula Ru(bpy)$_3$(ClO$_4$)$_2$·H$_2$O (calcd N = 10.68%, C = 45.80%, H = 3.30%) while the measured specific rotations ([α]$_D$ (Δ) = -880°, c = 0.059, H$_2$O; [α]$_D$ (Λ) = +825°, c = 0.039, H$_2$O) indicated optical purities (enantiomeric excess, ee) of 98% and 92% for the Δ-(-)$_D$ and Λ-(+)$_D$ perchlorate salts, respectively.[18] Δ,Λ-Co(phen)$_3$$^{2+}$ was prepared by adding 1,10-phenanthroline hydrate (5 mmol) into a

Figure 1. Idealized layer lattice structure of smectite clay depicting location of outer and inner ion-exchange sites. The approximate unit cell formulas for trioctahedral Na–hectorite and dioctahedral Na–montmorillonite may be written as Na$_{x'}y$H$_2$O[Li$_x$Mg$_{6-x}$](Si$_8$)O$_{20}$(OH,F)$_4$ and Na$_{x'}y$H$_2$O[Mg$_x$Al$_{4-x}$](Si$_8$)O$_{20}$(OH)$_4$, respectively, where $x \sim 0.7$ for the clays employed in the present work. Li/Mg in hectorite and Mg/Al in montmorillonite occupy the sandwiched octahedral sites while tetrahedral sites contain Si. The positions of oxygen (O) and OH/F (●) are also shown.

Figure 2. Optical isomers of Ru(bpy)$_3$$^{2+}$.
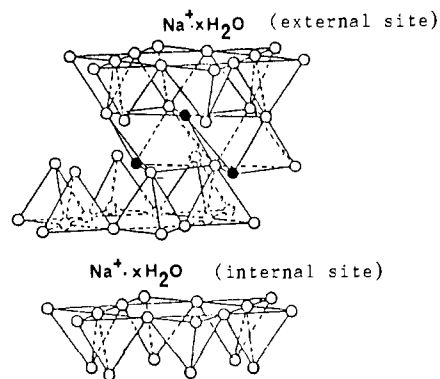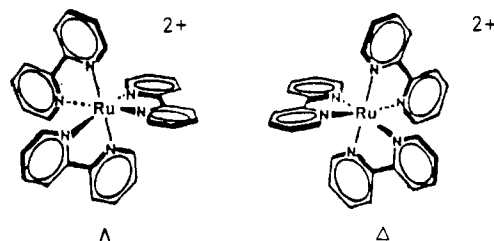
degassed solution of CoCl$_2$ (14.7 mmol) in 20 mL of H$_2$O.[20] The yellow solution was stirred under N$_2$ for 5 min, and the Co(II) complex subsequently precipitated by the addition of 10 mL of a saturated aqueous solution of NaClO$_4$. Following an additional 5 min of stirring, the precipitate was filtered, washed with cold water, and air dried (Anal. Obsd N = 10.27%, C = 52.46%, H = 2.98%; calcd (for Co(phen)$_3$-(ClO$_4$)$_2$H$_2$O) N = 10.29%, C = 52.98%, H = 3.18%). Δ,Λ-Co(phen)$_3$$^{3+}$ was prepared by oxidizing 0.86 mmol of the above Co(II) salt with 0.7 mmol of PbO$_2$ and 0.44 g of 12 N HCl in 73 mL of H$_2$O, at reflux temperature.[20] After 1 h an additional 0.7 mmol of PbO$_2$ was added, and the heating continued for another hour. The resultant solution was then filtered and passed through a Dowex 1×8-100 Cl$^-$ exchange column. The yellow eluant was precipitated with a saturated aqueous solution of NaClO$_4$, and the precipitate filtered, washed with cold water, and dried in air (Anal. Obsd N = 8.92%, C = 46.02%, H = 2.77%; calcd (for Co(phen)$_3$(ClO$_4$)$_3$·2H$_2$O) N = 8.99%, C = 46.28%, H = 2.99%). The dichloride salt of Δ,Λ-Zn(phen)$_3$$^{2+}$ was synthesized by the method of Reimann et al.[21] and found to be of satisfactory purity (Anal. Obsd N = 10.63%, C = 54.32%, H = 4.33%; calcd (for Zn(phen)$_3$Cl$_2$·6H$_2$O) N = 10.71%, C = 55.10%, H = 4.59%). Literature procedures were also employed for the synthesis and resolution of Λ-(+)$_D$-Ni(phen)$_3$$^{2+}$ ([α]$_D$ = 1322°, 90% ee)[22] and Λ(+)$_D$-Rh(phen)$_3$$^{3+}$ ([α]$_D$ = 808°).[23] Elemental analyses of the Ni(II) (N = 9.96%, C = 50.60%, H = 3.17%) and Rh(III) (N = 9.92%, C = 50.40%, H = 3.99%) salts indicated the molecular formulas Ni(phen)$_3$(ClO$_4$)$_2$·2H$_2$O (calcd N = 10.09%, C = 51.92%, H = 3.36%) and Rh(phen)$_3$Cl$_3$·5H$_2$O (calcd N = 10.00%, C = 51.40%, H = 4.04%). Absolute configurations of the above complexes have been previously assigned.[24]

Sodium dodecyl sulfate (SDS) and Nafion (5 wt % solution in alcohol) were obtained from ICI Specialty Chemicals (India) and Aldrich (U.K.), respectively. Other chemicals were of reagent grade, and triply distilled water was used in all experiments.

(12) Kotkar, D.; Joshi, V.; Ghosh, P. K. *Inorg. Chem.* **1986**, *25*, 4334.

(13) (a) Sutin, N.; Creutz, C. *Adv. Chem. Ser.* **1978**, *168*, 1. (b) Kalyanasundaram, K. *Coord. Chem. Rev.* **1982**, *46*, 159.

(14) (a) Abdo, S.; Canesson, P.; Cruz, M.; Fripiat, J. J.; Van Damme, H. *J. Phys. Chem.* **1981**, *85*, 797. (b) Krenske, D.; Abdo, S.; Van Damme, H.; Cruz, M.; Fripiat, J. J. *J. Phys. Chem.* **1980**, *84*, 2447. (c) Hahti, A.; Keravis, D.; Levitz, P.; Van Damme, H. *J. Chem. Soc., Faraday Trans. 2* **1984**, *80*, 67.

(15) (a) Thomas, J. K. *Acc. Chem. Res.* **1988**, *21*, 275, and references therein. (b) DellaGuardia, R.; Thomas, J. K. *J. Phys. Chem.* **1983**, *87*, 990.

(16) Schoonheydt, R. A.; de Pauw, P.; Vliers, D.; de Schrijver, F. C. *J. Phys. Chem.* **1984**, *88*, 5113.

(17) Braddock, J. N.; Meyer, T. J. *J. Am. Chem. Soc.* **1973**, *95*, 3158.

(18) Dwyer, F. P.; Gyarfas, E. C. *J. Proc. R. Soc., N.S.W.* **1949**, *83*, 174.

(19) Burstall, F. H. *J. Chem. Soc.* **1936**, 173.

(20) Johnson, W. L.; Geldard, J. F. *Inorg. Chem.* **1979**, *18*, 664.

(21) Reimann, C. W.; Block, S.; Perloff, A. *Inorg. Chem.* **1966**, *5*, 1185.

(22) Kauffman, G. B.; Takahashi, L. T. *Inorg. Synth.* **1966**, *8*, 227.

(23) Dollimore, L. S.; Gillard, R. D. *J. Chem. Soc., Dalton Trans.* **1973**, 933.

(24) (a) See *Inorg. Chem.* **1970**, *9*, 1 for nomenclature of optical isomers. (b) Mason, S. F.; Peart, B. J. *J. Chem. Soc., Dalton Trans.* **1973**, 949. (c) McCaffery, A. J.; Mason, S. F.; Norman, B. J. *J. Chem. Soc. A* **1969**, 1442.
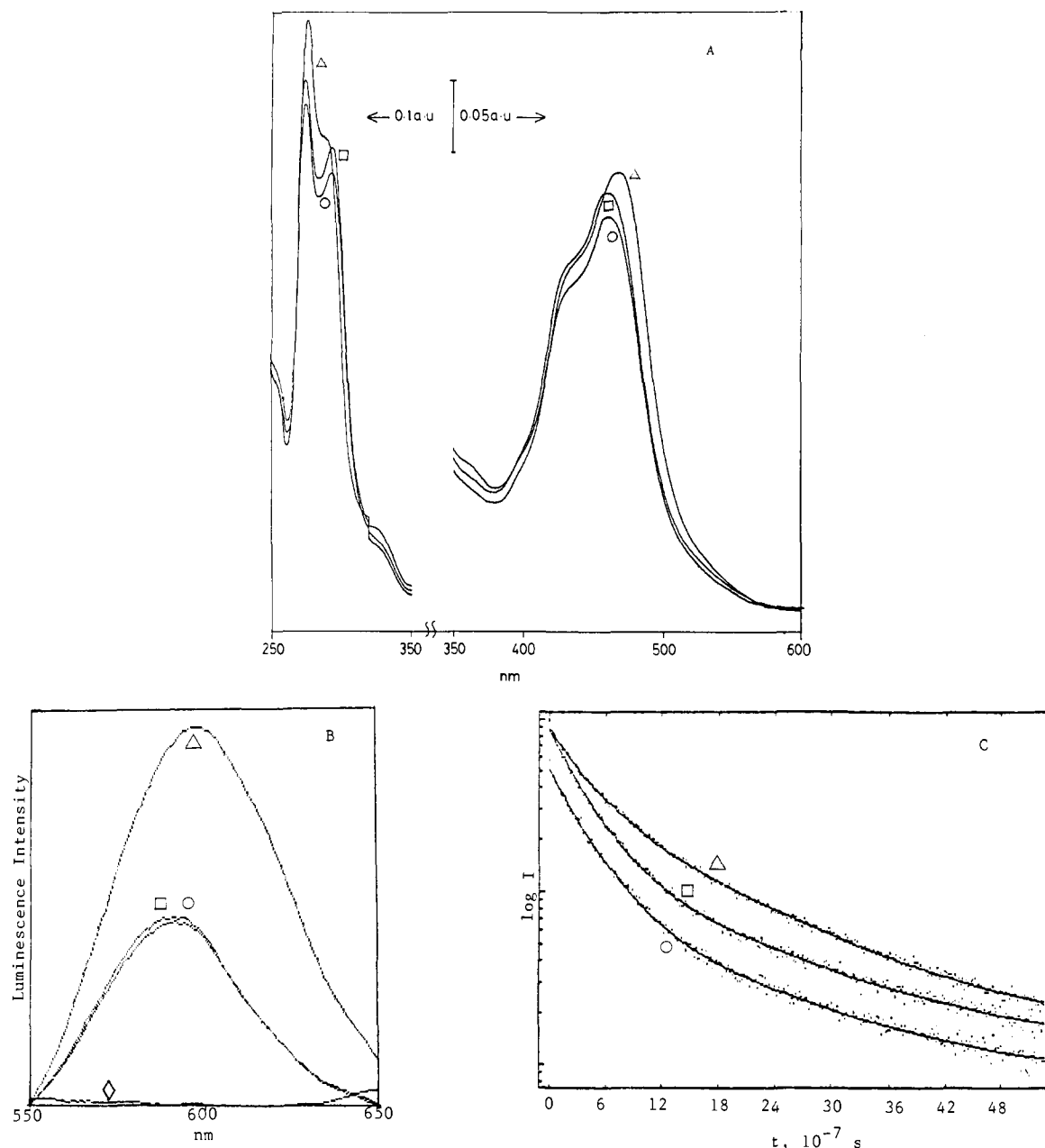
Figure 3. Absorption spectra (A), emission spectra (460-nm excitation; 5-nm excitation, and emission slits) (B), and time-resolved emission decay profiles (337-nm N_2 lamp excitation) (C) of ca. 1.7×10^{-5} M Λ-$(+)_D$- (O), Δ-$(-)_D$- ($\square$), and Δ,Λ-Ru(bpy)$_3{}^{2+}$ ($\triangle$) adsorbed on Na–hectorite clay (1 g/L). The peak count at $t \sim 0$ in (C) was 5795 (in 60 min) for Λ-$(+)_D$- and 10 199 (in 36 min) for Δ,Λ-Ru(bpy)$_3{}^{2+}$. Absorption spectra were recorded against a suitable clay reference, whose background emission spectrum ($\lozenge$) is also shown in (B). Δ,Λ-Ru(bpy)$_3{}^{2+}$ was prepared by premixing the Δ and Λ enantiomers prior to sorption. The cec of the clay dispersion was 1.02 mequiv/g.

Instrumentation. UV–vis absorption spectra were recorded on either a Pye-Unicam Model SP8-100 or a Shimadzu Model UV-160 spectrophotometer, while steady-state luminescence measurements were conducted on a Perkin-Elmer Model LS-5 spectrofluorimeter (side-on photomultiplier with S5 response) interfaced to a data station. Time-resolved luminescence studies were carried out on a single-photon-counting spectrometer (Model 199 M, Edinburgh Instruments, U.K.) fitted with a nitrogen discharge lamp (337 nm) and a computer (Model LSI 11/23, Plessey, U.K.) employing an appropriate reconvolution program. Optical rotations were measured on a digital polarimeter (Jasco DIP-140), and an elemental analyzer (Carlo Erba, Model 1106) was employed for carbon, hydrogen, and nitrogen analysis.

Results

Figure 1 shows the idealized structure of hectorite and montmorillonite clays. The clay samples were exchanged with sodium ions, purified, and yielded aqueous dispersions with good transparency. Their cation-exchange capacities (estimated through exchange adsorption with Λ-$(+)_D$-Ru(bpy)$_3{}^{2+}$) were in the range 0.95–1.05 mequiv/g. With a few exceptions, Ru(bpy)$_3{}^{2+}$ (Figure

2) and other poly(pyridyl) metal chelates employed in this work were synthesized and resolved following literature procedures, and their chemical and optical purities were found to be satisfactory. Absolute configurations of the chelates have been assigned by Mason and co-workers[24] on the basis of their ORD studies and the established Λ configuration of $(-)_D$-Fe(phen)$_3{}^{2+}$ and $(+)_D$-Ni(phen)$_3{}^{2+}$.[25,26] Upon addition of an aqueous metal chelate solution into a clay dispersion, the complex ions were rapidly and quantitatively adsorbed when their amount was less than the cec of the clay. The extent of adsorption was confirmed in all cases through spectral analysis of the supernatant following high-speed centrifugation of the dispersions.

Spectral Studies on Ru(bpy)$_3{}^{2+}$/Smectic Clays. Figure 3 shows the absorption, emission, and time-resolved emission decay profiles of Δ-$(-)_D$-, Λ-$(+)_D$-, and Δ,Λ-Ru(bpy)$_3{}^{2+}$ adsorbed at a ca. 3.5%

(25) Zalkin, A.; Templeton, D. H.; Veki, T. *Inorg. Chem.* **1973**, *12*, 1641.
(26) Butler, K. R.; Snow, M. R. *J. Chem. Soc. A* **1971**, 565.

Table I. UV–vis Absorption and Emission Spectral Data for Enantiomeric and Racemic $Ru(bpy)_3^{2+}$ (1×10^{-5} M) in Water, Micellar SDS, Nafion, and Smectite Clays

	absorption [λ_{max}/nm; (ϵ_{max}/10^4 M^{-1} cm^{-1})]		emission [λ_{max}/nm]	
medium[a]	enantiomer	racemate	enantiomer	racemate
water	452 (1.42)	452 (1.42)	598	598
	285 (7.90)	285 (7.90)		
SDS (17 mM)[b]	448 (1.45)	448 (1.45)	620	620
Nafion (10 g/L)[c]	451 (1.51)	451 (1.51)	598	598
	286 (8.74)	286 (8.74)		
SHCa-1 (1 g/L)[b]	461 (1.67)	470 (1.78)	590	597
	293 (4.18)	289 (4.22)		
	274 (4.56)	275 (5.30)		
GK129 (1 g/L)[b]	462 (1.61)	472 (1.68)	586	605
	294 (4.02)	289 (4.14)		
	272 (4.49)	273 (4.93)		
Vee Clay (1 g/L)[b]	462 (1.20)	470 (1.35)		
	295 (2.83)	290 (2.96)		
	278 (2.32)	280 (2.65)		

[a] Aqueous medium except for Nafion (2:1 MeOH/H₂O). [b] Spectra recorded on fresh solutions. [c] Spectra recorded after ca. 24 h.

Table II. Simulated Emission Kinetic Data of the Decay Profiles Shown in Figure 3C[a]

complex	α	τ_1^0, μs	$1 - \alpha$	τ_2^0, μs	χ^2
Λ-(+)$_D$	0.51	0.35	0.49	1.55	1.66
Δ-(-)$_D$	0.49	0.34	0.51	1.61	1.87
Δ,Λ	0.30	0.37	0.70	1.47	1.89

[a] Simulation studies were carried out with the decay function α exp-$(-t/\tau_1^0)$ + $(1 - \alpha)$ exp$(-t/\tau_2^0)$.

Table III. Relative Luminescence Intensities[a] of Enantiomeric and Racemic $Ru(bpy)_3^{2+*}$ as a Function of Loading Level in Na–Hectorite Clay (1 g/L)[b]

[$Ru(bpy)_3^{2+}$] $\times$ 10^5 M	% loading	$I_{\Delta(\text{or }\Lambda)}$	$I_{\Delta,\Lambda}$	$I_{\Delta,\Lambda}/I_{\Delta(\text{or }\Lambda)}$
0.5	1	30	81	2.74
1.0	2	56	136	2.40
2.0	4	99	197	1.98

[a] λ_{exc} = 460 nm (slit width = 5 nm), λ_{em} = 590 nm (slit width = 5 nm). [b] Cec of clay $\sim$1.02 mequiv/g.
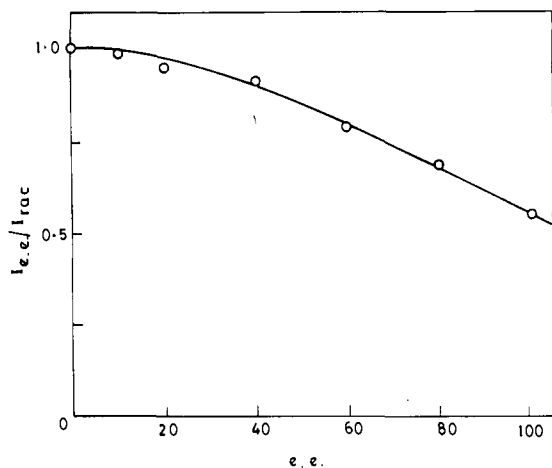
Figure 4. Plot of I_{ee}/I_{rac} vs ee, where ee = percent excess of Δ isomer in $Ru(bpy)_3^{2+}$ (1×10^{-5} M) adsorbed on Na–hectorite clay (1 g/L). I_{ee} = observed emission maximum for a given ee and I_{rac} = 1:1 racemate. Emission intensities were measured at 590 nm (slit width = 5 nm) employing 460-nm excitation (5-nm slit width).

loading on Na–hectorite (SHCa-1) clay (see also Tables I and II). The spectra were recorded at ambient (28–30 °C) temperatures, and they were not influenced by the nature of the counterion, identical results being obtained with bromide, chloride, and perchlorate salts.[27] As can be seen from Figure 3, the absorption and emission spectra of the two enantiomers were similar, but they differed considerably from those of the racemate,
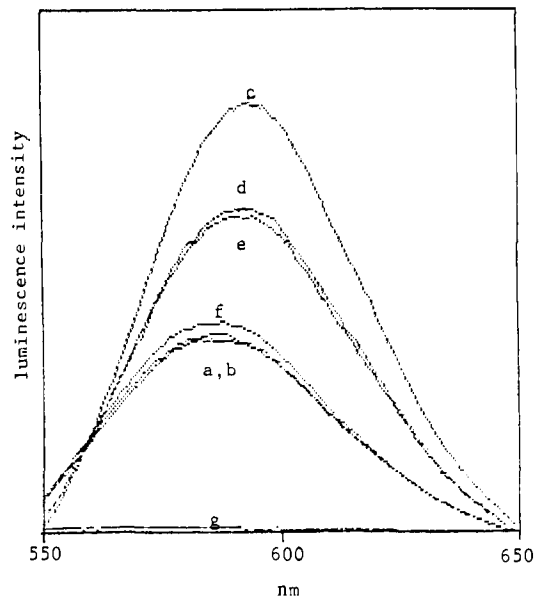
Figure 5. Emission spectra of 1.1×10^{-5} M Δ-(-)$_D$- (a), Λ-(+)$_D$- (b), and Δ,Λ-$Ru(bpy)_3^{2+}$ (c) adsorbed on 1 g/L Na–hectorite. Trace f shows the spectra obtained when equal volumes of a and b were mixed. Also shown in the figure are spectra for samples wherein 0.55×10^{-5} M Δ-(-)$_D$-Ru(II) was preadsorbed on 1 g/L Na–hectorite followed by addition of equimolar Λ-(+)$_D$, and vice versa (traces d and e). Trace g shows the background spectrum due to clay alone. All spectra were recorded after 3 h of equilibration time employing 460-nm excitation wavelength and 5-nm slit widths.

although such differences were not observed in water (Table I). However, the most prominent feature in Figure 3 is the ca. 2-fold difference in emission yield between enantiomer and racemate. This difference was also reflected in the luminescence decay profiles recorded at low excitation intensity, wherein the racemate exhibited a slower decay than either enantiomer alone. The time-resolved luminescence profiles could be satisfactorily simulated by using a double-exponential decay function, with lifetimes τ_1^0 and τ_2^0 and relative populations α and $(1 - \alpha)$, respectively (Table II). In agreement with previous observations, there was no significant change in luminescence yield when the solutions were purged with nitrogen.[14a,b] While the spectra shown in Figure 3 were recorded on fresh solutions, a small time-dependent increase in emission intensity was observed in some cases[2e] although the relative intensities of enantiomer and racemate remained nearly unchanged. The luminescence intensity ratio [$I_{\Delta,\Lambda}/I_{\Delta(\text{or }\Lambda)}$] was studied as a function of loading level. As shown in Table III, this ratio increased with decreased loading, other conditions being the same. Changes in luminescence intensity were also monitored by varying the optical purity of Δ-(-)$_D$-$Ru(bpy)_3^{2+}$, and Figure 4 shows a plot of the decrease in emission intensity with increasing optical purity. Some insight into the adsorption process was obtained by altering the mode of addition of chelate ions into the clay dispersion. Figure 5 shows emission spectra recorded for pure enantiomers (traces a and b) and for premixed racemate (trace c), while traces d and e correspond to a two-step sequence of racemate formation wherein one of the enantiomers was added first into the clay dispersion followed by addition of the second enantiomer after 10 min. (This time interval ensured complete adsorption of the first enantiomer prior to addition of its antipode). Trace f was obtained when the enantiomers were separately adsorbed on clay and the solutions subsequently mixed. As can be seen from the figure, even after an equilibration time of ca. 3 h, the luminescence intensities of d and e were markedly less than

(27) Δ,Λ-$Ru(bpy)_3^{2+}$ was prepared by premixing the pure enantiomers prior to sorption. All samples were prepared through rapid addition of the aqueous solution containing chelate ions into the clay dispersion. The results were similar when the mode of addition was reversed. Such considerations are nevertheless important when the adsorption process is rapid (<0.1 s), as in the present case.

Table IV. Estimated K_{SV} (Stern–Volmer Constant) and k_q (Apparent Bimolecular Rate Constant) for the Quenching of Δ-(−)$_D$-, Λ-(+)$_D$-, and Δ,Λ-Ru(bpy)$_3^{2+*}$ by Coadsorbed M(phen)$_3^{n+}$ Quenchers[a]

quencher	K_{SV}, M^{-1}			$k_q \times 10^{-8}$, M^{-1} s^{-1}		
	Λ-(+)$_D$	Δ-(−)$_D$	Δ,Λ	Λ-(+)$_D$	Δ-(−)$_D$	Δ,Λ
Δ,Λ-Co(phen)$_3^{2+}$	200		357	3.6		4.6
Δ,Λ-Co(phen)$_3^{3+}$	120		320	2.1		4.1
Λ-(+)$_D$-Ni(phen)$_3^{2+}$	5.9	23.8	55.9	0.10	0.41	0.71
Λ-(+)$_D$-Rh(phen)$_3^{3+}$	3.56	17.8	34.5	0.06	0.31	0.44

[a] Calculations were based on eq 1, the data being obtained from Table II and Figures 8 and 11. The concentration scale in the figures was corrected, assuming complete (but random) adsorption of the quencher on clay and a clay density of 2 g/L.
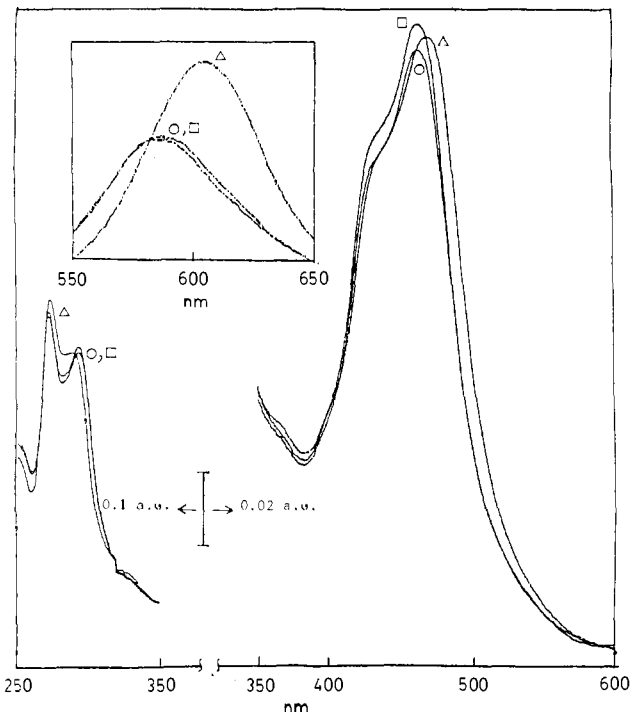
Figure 6. Absorption spectra of ca. 1.1×10^{-5} M Λ-(+)$_D$- (O), Δ-(−)$_D$- (□), and Δ,Λ-Ru(bpy)$_3^{2+}$ (△) adsorbed on 1 g/L Na–montmorillonite (GK 129) clay. The spectra were recorded against a suitable clay reference. The inset shows the corresponding luminescence spectra (460-nm excitation; excitation and emission slit widths 5 and 10 nm, respectively). Δ,Λ-Ru(bpy)$_3^{2+}$ was prepared by premixing the isomers prior to sorption. The cec of the clay dispersion was ~0.94 mequiv/g.
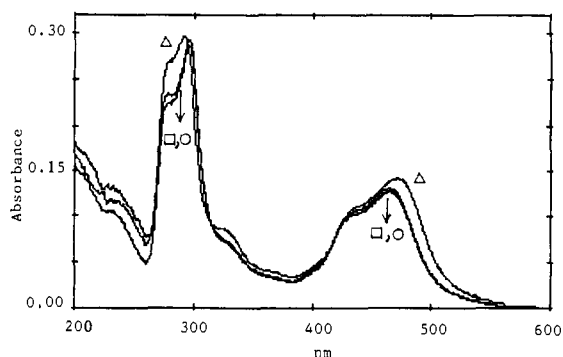
Figure 7. Absorption spectra of 1×10^{-5} M Λ-(+)$_D$- (O), Δ-(−)$_D$- (□), and Δ,Λ-Ru(bpy)$_3^{2+}$ (△) adsorbed on 1 g/L Na–montmorillonite (Vee Clay WE). The spectra were recorded against a suitable clay reference. Δ,Λ-Ru(bpy)$_3^{2+}$ was prepared by premixing the enantiomers prior to sorption. The cec of the clay was ~1.04 mequiv/g.

that of c, while f resembled the pure enantiomers a and b.

Absorption spectral results similar to those reported above for Na–hectorite were also observed on montmorillonite clays. Spectra of two such clays are shown in Figures 6 (GK 129) and 7 (Vee Clay; see also Table I). On the other hand, emission spectral results differed considerably: Thus, emission intensities were lower on montmorillonite clay, the value being 5–7 times smaller on GK 129 clay[10a,15a] and negligibly small on Vee Clay. As shown in the
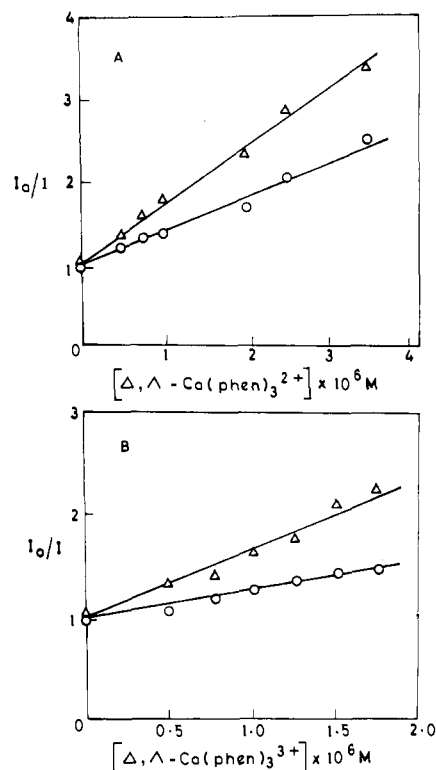
Figure 8. Stern–Volmer plots for the quenching of 1×10^{-5} M Λ-(+)$_D$- (O) and Δ,Λ-Ru(bpy)$_3^{2+*}$ (△) by Δ,Λ-Co(phen)$_3^{2+}$ (A) and Δ,Λ-Co-(phen)$_3^{3+}$ (B), coadsorbed on Na–hectorite clay. The complexes were premixed prior to sorption on clay.

Table V. Effect of M(phen)$_3^{n+}$ Coadsorbates on the MLCT Absorption Maximum of Δ-(−)$_D$-, Λ-(+)$_D$-, and Δ,Λ-Ru(bpy)$_3^{2+}$ Adsorbed on Na–Hectorite Clay (1 g/L)

[Ru(bpy)$_3^{2+}$] × 10^5 M	M(phen)$_3^{n+}$ [×10^5 M]	$\lambda_{max(MLCT)}$, nm		
		Λ-(+)$_D$	Δ-(−)$_D$	Δ,Λ
1.0		462	462	470
1.0	Δ,Λ-Co(phen)$_3^{2+}$ [1.0]	466	466	466
1.0	Δ,Λ-Zn(phen)$_3^{2+}$ [1.0]	465	465	465
1.2	Λ-(+)$_D$Ni(phen)$_3^{2+}$ [1.3]	462	465	467
1.2	Λ-(+)$_D$-Rh(phen)$_3^{3+}$ [1.5]	462	466	468

inset of Figure 6, there were pronounced differences in the spectral profiles as well, the differences in peak maximum between enantiomer and racemate being 7 nm for Na–hectorite and 19 nm for GK 129 montmorillonite clay. However, the relative emission intensities were similar in the two clays.

While spectral differences between enantiomeric and racemic Ru(bpy)$_3^{2+}$ were a common feature in all the smectite clays studied, such differences were not found on other supports. Thus absorption and emission spectra of the two forms of Ru(bpy)$_3^{2+}$ were the same in micellar SDS,[28] adsorption of the chelate on the micelle being evident from the ca. 20-nm red shift in emission maximum (Table I). Similarly, the spectra of Δ-(−)$_D$-, Λ-(+)$_D$-, and Δ,Λ-Ru(bpy)$_3^{2+}$ were identical in a 2:1 MeOH/H$_2$O solution

(28) (a) Schmehl, R. H.; Whitten, D. G. *J. Am. Chem. Soc.* **1980**, *102*, 1938. (b) Kaifer, A. E.; Bard, A. J. *J. Phys. Chem.* **1985**, *89*, 4876.
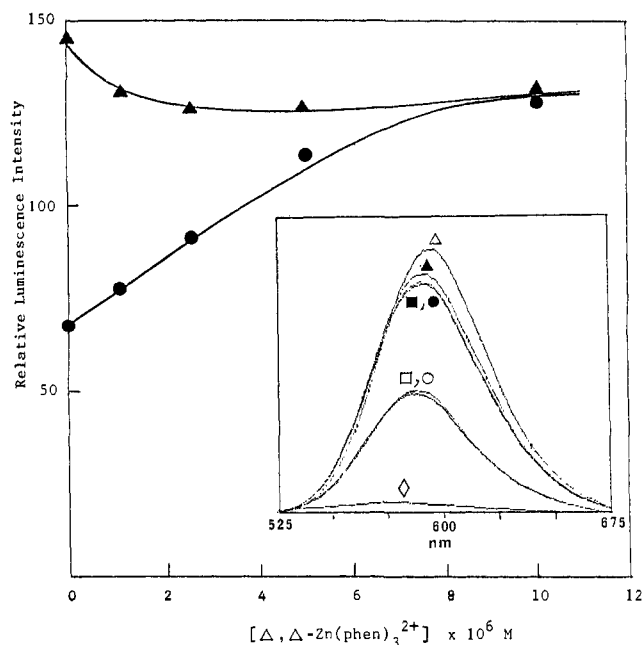
Figure 9. Plot of peak luminescence intensity of 1×10^{-5} M $Ru(bpy)_3^{2+*}$ [Λ-(+)$_D$- ($\bullet$); Δ,Λ- ($\blacktriangle$)] as a function of [Δ,Λ-Zn(phen)$_3^{2+}$] coadsorbed on Na–hectorite clay (1 g/L). The inset shows the emission spectra (460-nm excitation; 5-nm excitation and emission slits) of the enantiomeric and racemic $Ru(bpy)_3^{2+*}$ complexes in the absence [Λ-(+)$_D$ (O), Δ-(-)$_D$ ($\square$), Δ,Λ- ($\triangle$)] and presence [Λ-(+)$_D$ ($\bullet$), Δ-(-)$_D$ ($\blacksquare$), Δ,Λ- ($\blacktriangle$)] of 2×10^{-5} M coadsorbed Δ,Λ-Zn(phen)$_3^{2+}$. The background spectrum of clay ($\lozenge$) is also shown.

containing Nafion polymer (Table I). While direct proof of association between the Ru(II) chelate and Nafion was not obtained in our work, previous studies employing Nafion films have demonstrated that $Ru(bpy)_3^{2+}$ is strongly held in the polymer matrix.[29]

Effect of M(phen)$_3^{n+}$ Coadsorbates on Ru(bpy)$_3^{2+}$ Absorption and Emission. Figure 8 shows Stern–Volmer plots for the quenching of Λ-(+)$_D$- and Δ,Λ-Ru(bpy)$_3^{2+*}$ by coadsorbed Δ,Λ-Co(phen)$_3^{2+}$ and Δ,Λ-Co(phen)$_3^{3+}$ in Na–hectorite. The plot of Δ-(-)$_D$-Ru(II) was similar to that of Λ-(+)$_D$-Ru(II) and has been omitted for the sake of clarity. Note that unlike in normal solution quenching studies, wherein the quencher concentration is at least 1–2 orders of magnitude higher than that of the molecule whose excited state is subjected to quenching, the Stern–Volmer plots in Figure 8 were obtained with [Co(II)] and [Co(III)] < [Ru(II)]. Kinetic parameters corresponding to the above plots are shown in Table IV. The apparent rate constant, k_q, was estimated by using the relation shown in eq 1, where K_{SV} is the Stern–Volmer

$$k_q = K_{SV}[\alpha/\tau_1^0 + (1 - \alpha)/\tau_2^0] \qquad (1)$$

constant, and α, $(1 - \alpha)$, τ_1^0, and τ_2^0 have their usual meanings (Table II). For $\tau_1^0 = \tau_2^0 = \tau^0$, eq 1 reduces to $k_q = K_{SV}/\tau^0$.[30] The concentrating effect of the clay was taken into account in the computation of K_{SV}.[31] The results in Table IV suggest that racemic $Ru(bpy)_3^{2+*}$ is quenched more effectively by the Co(II) and Co(III) coadsorbates and that the former is a slightly better quencher than the latter within the clay matrix. Curiously, the MLCT absorption profiles of the enantiomeric and racemic Ru(II) chelates became nearly identical in the presence of 1 equiv of Co(phen)$_3^{2+}$ (Table V), although differences between the two forms (Figure 3A) were evident in the absence of coadsorbate. To shed further light on binding-state perturbations—in particular their effect on the excited-state of Ru(II)—luminescence spectra of Δ-(-)$_D$-, Λ-(+)$_D$- and Δ,Λ-Ru(bpy)$_3^{2+*}$ were recorded with

(29) Rubinstein, I.; Bard, A. J. *J. Am. Chem. Soc.* **1980**, *102*, 6641.

(30) Turro, N. J. *Modern Molecular Photochemistry*; Benjamin Cummings: CA, 1978; p 248.

(31) Corrected concentrations of quencher were estimated from the known weight of clay in solution and an assumed density of 2 g/mL.[15b]
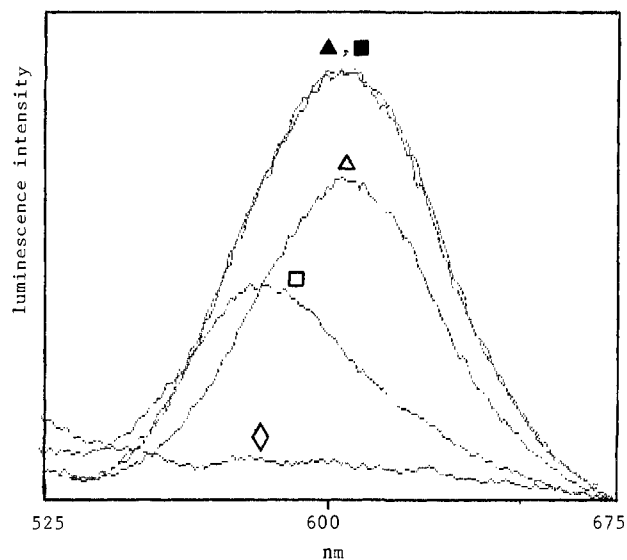
Figure 10. Luminescence spectra of 1×10^{-5} M $Ru(bpy)_3^{2+}$ in the absence [Δ-(-)$_D$- ($\square$), Δ,Λ- ($\triangle$)] and presence [Δ-(-)$_D$- ($\blacksquare$), Δ,Λ- ($\blacktriangle$)] of 2×10^{-5} M Δ,Λ-Zn(phen)$_3^{2+}$ coadsorbed on Na–montmorillonite (GK 129) clay (1 g/L). The complexes were premixed prior to sorption. Excitation wavelength was 460 nm, and the excitation and emission slits were both 5 nm. The background spectrum of clay ($\lozenge$) is also shown.
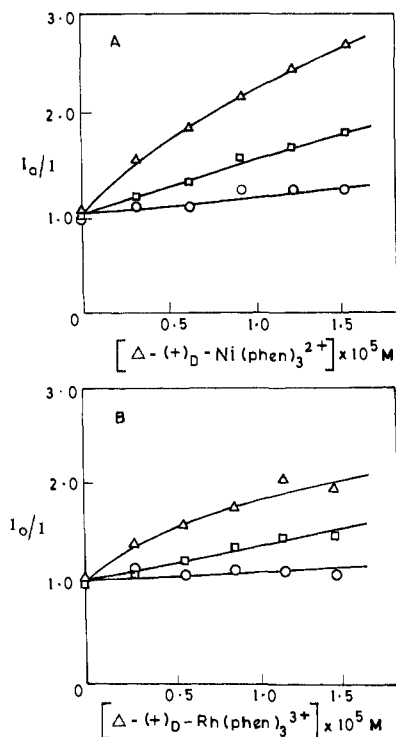
Figure 11. Stern–Volmer plots for the quenching of 1.2×10^{-5} M Λ-(+)$_D$- (O), Δ-(-)$_D$- ($\square$), and Δ,Λ-Ru(bpy)$_3^{2+*}$ ($\triangle$) by Λ-(+)$_D$-Ni(phen)$_3^{2+}$ (A) and Λ-(+)$_D$-Rh(phen)$_3^{3+}$ (B) coadsorbed on Na–hectorite clay (1 g/L). Solutions of the Ru(II) complex and quencher were premixed prior to sorption.

Δ,Λ-Zn(phen)$_3^{2+}$ as coadsorbate. The latter complex has the unique advantage of being a "nonquencher" which is otherwise structurally analogous to Co(phen)$_3^{2+}$. As shown in Figure 9, the emission of Δ-(-)$_D$- and Λ-(+)$_D$-Ru(bpy)$_3^{2+*}$ increased with increasing Zn(II) while that of the racemate remained nearly unchanged. With [Zn(II)]/[Ru(II)] = 2, the emission spectra of the enantiomeric and racemic forms of Ru(II) were nearly identical, both in intensity and in profile (see inset in Figure 9). Changes in the MLCT absorption spectra were also observed and are listed in Table V. The results with Zn(II) were not unique to Na–hectorite, analogous changes in emission being found on

GK 129 montmorillonite clay (Figure 10). Quenching studies were also carried out by using two optically active $M(phen)_3^{n+}$ quenchers. Figure 11 shows the Stern–Volmer plots of Λ-$(-)_D$-, Λ-$(+)_D$-, and Δ,Λ-Ru(bpy)$_3^{2+}$ obtained by using Λ-$(+)_D$-Ni-(phen)$_3^{2+}$ and Λ-$(+)_D$-Rh(phen)$_3^{3+}$ as quenchers. Apparent k_q values and shifts in the MLCT absorption maximum of Ru(II) are presented in Tables IV and V, respectively. The apparent quenching efficiencies with the Λ quenchers followed the trend Δ,Λ-Ru(bpy)$_3^{2+*}$ > Λ-$(-)_D$-Ru(bpy)$_3^{2+*}$ > Λ-$(+)_D$-Ru(bpy)$_3^{2+*}$.

Discussion

Smectite Clay Structure. Montmorillonite and hectorite (Figure 1) belong to the family of expandable three-layer minerals (smectites) in which an octahedral layer of alumina/magnesia shares oxygen atoms with tetrahedral silica layers, one on either side. In a typical mineral several such composite layers (platelets) are held together by van der Waals forces as a face-to-face aggregate. The van der Waals energy, V_A (erg cm^{-2}) between two layers may be expressed by eq 2, where d is the half-distance

$$V_A = -(A/48\pi)[1/d^2 + 1/(d + \Delta)^2 - 2/(d + \Delta/2)^2] \quad (2)$$

between the plates, Δ is the unit layer thickness (ca. 9.6 Å), and $A \sim 10^{-12}$.[32] The charge imbalance in these clays originates from isomorphos substitution of cations in the octahedral layer with lower valent metal ions. Thus, montmorillonite and hectorite (cec ~ 1 mequiv/g; total surface area ~ 750 m^2/g) may be derived from pyrophyllite [Al$_4$Si$_8$O$_{20}$(OH)$_4$] and talc [Mg$_6$Si$_8$O$_{20}$(OH)$_4$] through partial replacement of Al^{3+} and Mg^{2+} with Mg^{2+} and Li$^+$, respectively. Isoelectric substitution of Al^{3+} with Fe^{3+} also occurs to varying extents in montmorillonite clays; facile oxidative quenching by lattice Fe^{3+} is to a large extent responsible for the lower emission of Ru(bpy)$_3^{2+*}$ in montmorillonite clays than in hectorite.[10a,14–16] When the above clays are ion-exchanged with Na$^+$, there is a marked interlayer swelling, leading to eventual delamination of platelets due to a decrease in V_A (eq 2) and ease of dispersibility in water. The delamination process is however rarely complete, so that dispersed particles offer both internal and external sites for adsorption (Figure 1), the ratio of the two being proportional to the aggregation number. Consequently, metal chelates adsorbed on such a particle might encounter more than one environment.[2e,15a] The adsorption process may be further complicated as a result of clay matrix inhomogeneity[33] and time-dependent aggregation of clay particles. The latter process might account for the slight changes in the emission intensity of adsorbed Ru(bpy)$_3^{2+*}$ with aging.[2e]

Racemic Interactions. The cationic poly(pyridyl) metal chelates employed in this work are held strongly on the smectite clays, presumably by a combination of electrostatic and ion–dipole interactions.[2a] Yamagishi had indicated that while a maximum of one exchange equivalent of $(-)_D$- or $(+)_D$-Fe(phen)$_3^{2+}$ can be adsorbed on montmorillonite clays, twice this amount is adsorbed when the Fe(II) complex is added as a racemate.[2c] Evidently, the above result is not sufficiently general since Λ-$(+)_D$-, Δ-$(-)_D$-, and Δ,Λ-Ru(bpy)$_3^{2+}$ adsorb to the same extent—i.e., the exchange equivalent—on the smectite clays employed in this work. The absorption spectrum of lightly loaded Δ,Λ-Ru(bpy)$_3^{2+}$ was similar for all the clays investigated and in good accord with published data.[15a] To eliminate possible ambiguity in the interpretation of our results, the Ru(II) racemate was reconstituted from pure enantiomers, although identical results were obtained with authentic samples of the racemic complex. The pronounced changes in absorption spectrum upon adsorption on clay (Table I) have been ascribed to strong interactions between chelate and support: It has been proposed that the structure of the chelate undergoes distortion upon binding with concomitant destablization of the +2 oxidation state of the central metal ion.[14a,15] Resonance Raman studies, however, have failed to provide evidence of extensive distortion.[10a] Interpretation of the absorption spectral changes

$\nu_a > \nu_a' > \nu_a''$

$\nu_e' > \nu_e \nsucc \nu_e''$
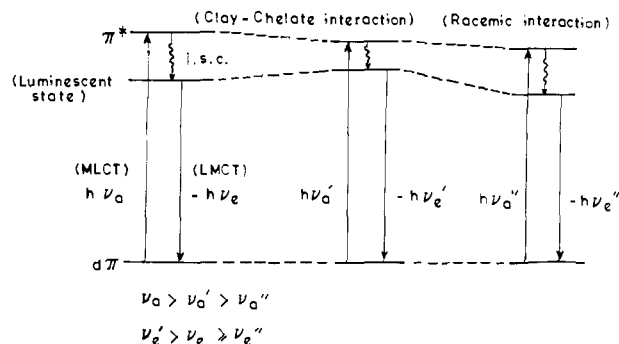
Figure 12. Schematic representation of ligand orbital energy perturbations corresponding to observed shifts in the metal-to-ligand charge-transfer (MLCT) absorption and ligand-to-metal charge-transfer (LMCT) emission spectra of enantiomeric and racemic Ru(bpy)$_3^{2+}$ upon adsorption on smectite clay. (Ru(II) being deeply buried in the complex, the energies of metal-localized orbitals have been assumed to remain unchanged.) Spectral shifts of the adsorbed enantiomers have been ascribed exclusively to clay–chelate interactions, while those of the adsorbed racemate have been ascribed to both clay–chelate and antipode-antipode (racemic) interactions. Intersystem crossing to the partially spin-forbidden emitting (ϕ_{soln} (25 °C) ~ 0.04)[13b] state is denoted by isc.

on the basis of clay–chelate interactions alone may be difficult in view of the data in Table I. Our results reveal that the absorption spectra of enantiomer and racemate are different even at low loading and that the spectrum of the latter is therefore best understood in terms of two effects: clay–chelate interaction and spontaneous antipode–antipode (racemic) interaction. These effects are additive for the MLCT absorption, while interpretation of the ligand-centered $\pi-\pi^*$ transition is more complex. The above interactions have opposite effects on the emission spectrum: adsorption of pure enantiomers raises the energy of the emission maximum while racemic interactions produce a bathochromic shift (Figures 3 and 6, Table I). The contrasting nature of the absorption (MLCT) and emission trends is schematically shown in Figure 12, it being assumed that the observed shifts in peak positions are exclusively due to perturbations in the energies of ligand-centered orbitals. Such an assumption appears reasonable since the central metal ion is deeply buried in the complex. It can be seen from Figure 12 that opposing effects account for the otherwise surprising lack of change in the emission spectrum of Δ,Λ-Ru(bpy)$_3^{2+*}$–hectorite (Figure 3B).[10a] Our spectral studies also suggest that the correlation between emission λ_{max} and clay charge density reported by Schoonheydt et al.[16] must be viewed with skepticism since a comparison of the data for Na–montmorillonite (GK 129) and Na–hectorite (SHCa-1) in Table I indicates that the trends are opposite for enantiomer and racemate.

From the above discussion, Ru(II) chelates of opposite handedness interact spontaneously in clay while chelates of similar handedness do not, and the observed spectral shifts are a direct measure of the strength of such "permanent" interactions. Relative steady-state luminescence intensity measurements also indicate dissimilarities in the adsorption modes of the enantiomeric and racemic forms, on both Na–hectorite (Figure 3b) and Na–montmorillonite (Figure 6).[34] Such differences are also reflected in the single-photon-counting flash excitation studies. Thus, when the data acquisition period is maintained constant, the accumulated counts at $t \sim 0$ are ca. 2–3 times higher for the racemate than for the enantiomer. Statistically, this would suggest that compared to the adsorbed enantiomers, a higher fraction of excited racemates are in the emitting state. Additionally, the time-resolved emission profiles (Figure 3C)—which are complex even under conditions that would preclude self-annihilation of excited states[10a]—indicate a slower luminescence decay of adsorbed racemates. On the other hand, the traces of the two enantiomers are nearly superimposable (see also data in Table II), minor variations being ascribed to differences in optical purity. The decay profiles could be fit by

(32) Van Olphen, H. *An Introduction to Clay Colloid Chemistry*; Wiley: New York, 1977.

(33) Lagaly, G.; Weiss, A. *Proc. Int. Clay. Conf. 1975*; Bailey, S. W., Ed.; Applied Publishing: Wilmette IL; pp 157–172.

(34) Although not relevant to the present work, we would like to point out a recent report on clay–intercalated methyl viologen (MV^{2+}) emission (Villemure. G.; Detellier, C.; Szabo, A. G. *J. Am. Chem. Soc.* **1986**, *108*, 4658).

Poly(pyridyl) Metal Chelates

J. Am. Chem. Soc., Vol. 111, No. 15, 1989 5611
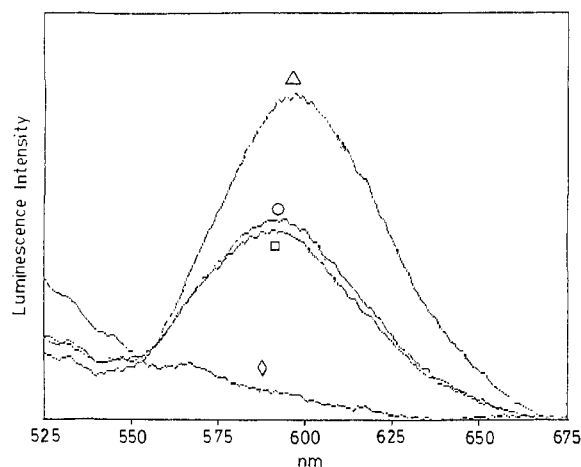
Figure 13. Luminescence spectra of 1×10^{-5} M Λ-(+)$_D$- (O), Δ-(-)$_D$- ($\square$), and Δ,Λ-Ru(bpy)$_3$$^{2+}$* ($\triangle$) adsorbed on kaolinite clay (0.7 g/L). The background spectrum of the clay alone ($\diamond$) is also shown (λ_{exc} = 450 nm; 5-nm excitation and emission slits).

employing a double-exponential function, and the data in Table II suggest that the values of τ_1^0 and τ_2^0 are nearly identical for the enantiomers and racemate while the relative populations $[\alpha/(1 - \alpha)]$ are changed. While simulation of the emission traces shown in Figure 3C are fraught with uncertainties—e.g., the actual rate equation may be more complex and/or the similarities in lifetimes may be merely coincidental—it is nevertheless tempting to propose that the Ru(bpy)$_3$$^{2+}$ ions encounter two distinctly different adsorption sites on clay, $[\alpha/(1 - \alpha)]$ being influenced by "transient" interactions between optical antipodes. Since ground- and excited-state properties might both be perturbed by the environment, the net absorption and emission spectra of enantiomer and racemate could differ as an indirect consequence of such interactions. Turro and co-workers have proposed that the luminescence yield of Ru(bpy)$_3$$^{2+}$* may vary substantially on internal and external sites.[2e] Might it then be that "transient" interactions perturb the relative occupancies of inner and outer sites leading to the large difference in emission yield between enantiomers and racemate? To shed light on this possibility, some experiments were carried out using kaolinite, a nonexpanding clay offering only external sites for exchange adsorption.[32,35a] The MLCT absorption profiles of Δ-(-)$_D$-, Λ-(+)$_D$-, and Δ,Λ-Ru(bpy)$_3$$^{2+}$ were similar on kaolinite, the absorption maximum (λ_{max} = 463 nm)[35b] closely resembling that of the enantiomers on smectite clays (Table I). However, differences in the binding modes of the enantiomeric and racemic forms were apparent from their π–π* absorption profiles. More importantly, emission spectral results also differed, and the ca. 2-fold higher emission intensity of Δ,Λ-Ru(bpy)$_3$$^{2+}$* was observed on kaolinite clay as well (Figure 13). Thus the luminescence spectral results observed on smectite clay cannot be explained in terms of variations in the occupancy ratio of internal and external sites. We tentatively propose that spectral shifts—and accompanying differences in molar absorptivity and emission quantum yield—between enantiomers and racemate on smectite clay are indeed a measure of "permanent" interactions between optical antipodes,[11,36a] the interaction energy being estimated to be in the range 1.0–1.4 kcal/mol. We note that ev-

idence of spontaneous aggregation of Δ,Λ-Ru(bpy)$_3$$^{2+}$, indicative of molecule–molecule interaction, has been previously reported, although such aggregation was not attributed, as such, to racemic interactions.[10a,36b]

Without exception, the layered clays investigated in this study promote the mutual recognition of Δ-(-)$_D$- and Λ-(+)$_D$-Ru-(bpy)$_3$$^{2+}$. In contrast, there is no evidence of selective interactions when these same ions are supported on micellar SDS and Nafion. Why are clays such good sorters of chiral molecules? Salem has recently computed the differential interaction energy between two chiral tetrahedral molecules in the limit of free relative molecular rotation.[37] While the "chirality forces" reported by Salem are extremely small in magnitude, it would be reasonable to speculate that chiral recognition may be enhanced by aligning molecules in selective configurations and by ensuring adequate interaction between them, e.g., through π–π overlap.[38,39] X-ray studies have previously established that poly(pyridyl) metal chelates adsorb on clay with their C_3 axis perpendicular to the clay plane.[2c,9] Polarized luminescence measurements have also provided evidence of restricted rotation of Δ,Λ-Ru(bpy)$_3$$^{2+}$ in montmorillonite and kaolinite clays.[15] Clays therefore serve as suitable matrices for preferential alignment of the above molecules, thereby facilitating chiral recognition. The clay–solution interface also appears to play some role in the sorting process. As shown in Figure 5, the spectral results were not the same when the enantiomers were premixed prior to sorption (trace c) and when they were sequentially added into the clay dispersion. The spectral variation probably corresponds to differences in the degree of aggregation within the clay layer: In the first case racemic pairing at the clay–solution interface might facilitate formation of extended aggregates with alternating Δ and Λ. In the second case, addition of a pure enantiomer perhaps yields a more random distribution of the adsorbed chelate. Subsequent addition of its antipode leads to racemic pairing, albeit with limited aggregation. Note that equilibration through the process of desorption and adsorption appears to be exceedingly slow, as is evident from a comparison of traces, a, b, and f in Figure 5.

Pseudoracemic Interactions and Quenching Processes in Clay Layers. Coadsorbed M(phen)$_3$$^{n+}$ chelates perturb the binding state of Ru(bpy)$_3$$^{2+}$. This is evident from the absorption spectral data in Table V but is most conclusively demonstrated by our emission spectral studies employing Δ,Λ-Zn(phen)$_3$$^{2+}$ as coadsorbate (Figures 9 and 10).[40] Binding-state perturbations are presumably induced by "pseudoracemic" interactions between the optical antipodes of Ru(bpy)$_3$$^{2+}$ and Zn(phen)$_3$$^{2+}$. Such interactions, which are anticipated to occur via π–π overlap, are evidently strong enough to dislodge the racemic interaction (also through π–π overlap) observed for Δ,Λ-Ru(bpy)$_3$$^{2+}$ in the absence of coadsorbate; as a result, the binding states of enantiomeric and racemic Ru(bpy)$_3$$^{2+}$ become essentially alike in the presence of a stoichiometric equivalent of Δ,Λ-Zn(phen)$_3$$^{2+}$ (Figures 9 and 10).

The tris(phenanthroline) chelates of Co(II), Co(III), Ni(II), and Rh(III) quench the excited state of adsorbed Ru(bpy)$_3$$^{2+}$, albeit with varying efficiencies (Figures 8 and 11, Table IV). While Co(phen)$_3$$^{3+}$ and Rh(phen)$_3$$^{3+}$ reportedly quench the excited state of Ru(bpy)$_3$$^{2+}$ via oxidative electron transfer,[13b] an energy-transfer quenching mechanism has been proposed for Co-(phen)$_3$$^{2+}$.[41] To our knowledge, there is no previous report of excited-state quenching with Ni(phen)$_3$$^{2+}$.[42] Due to the lack of accessible redox states in Ni(phen)$_3$$^{2+}$, the quenching mechanism

(35) (a) Hydrite PX grade kaolinite from Georgia Kaolin company was treated with NaCl, as described for other clays (see the Experimental Section), and the salt-free clay dispersion was centrifuged at 2000 rpm to remove heavier particles. (b) This value is in good accord with the reported value (λ_{max} = 465 nm) of Δ,Λ-Ru(bpy)$_3$$^{2+}$ on kaolinite.[15b]

(36) (a) Other forms of inhomogeneity in the clay matrix, e.g., site-to-site variations in charge density, must however be taken into account to evolve a fuller understanding of the spectral behavior of adsorbed chelates.[33] Clearly, the adsorbed chelates are highly sensitive luminescent probes of even minor structural and electronic differences such as those that might exist between Na–hectorite and Na–montmorillonite. (b) There is no hard evidence to suggest that enantiomeric Ru(bpy)$_3$$^{2+}$ does not aggregate in the clay layers. Time-resolved emission studies at high excitation intensity may provide a more definitive answer in this regard.[10a]

(37) Salem, L.; Chapuisat, X.; Segal, G.; Hilberty, P. C.; Minot, C.; Leforestier, C.; Sautet, P. *J. Am. Chem. Soc.* **1987**, *109*, 2887.

(38) Lipkowitz, K. B.; Demeter, D. A.; Zegarra, R.; Larter, R.; Darden, T. *J. Am. Chem. Soc.* **1988**, *110*, 3446.

(39) (a) Pirkle, W. H.; Hyun, M. H.; Banks, B. *J. Chromatogr.* **1984**, *316*, 585. (b) Pirkle, W. H.; Finn, J. M.; Hamper, B. C.; Schreiner, J.; Pribish, J. R. In *Asymmetric Reactions and Processes in Chemistry*; Eliel, E., Otsuka, S., Eds.; ACS Symposium Series No. 185; American Chemical Society: Washington DC, 1982; p 256.

(40) It has been previously shown that Δ,Λ-Zn(phen)$_3$$^{2+}$ suppresses the triplet–triplet annihilation of clay-adsorbed Δ,Λ-Ru(bpy)$_3$$^{2+}$* at high excitation intensity.[10a]

(41) Creutz, C.; Sutin, N. *Inorg. Chem.* **1976**, *15*, 496.

for this chelate must also involve energy transfer. In water, the bimolecular quenching rate constant obtained by using Co-$(phen)_3^{2+}$ as quencher ($k_q = 8.9 \times 10^8$ M^{-1} s^{-1}) is less than that of $Co(phen)_3^{3+}$ (3.0×10^9 M^{-1} s^{-1}) and comparable to that of $Rh(phen)_3^{3+}$ (6.8×10^8 M^{-1} s^{-1}). In clay, however, quenching was most efficient with Δ,Λ-$Co(phen)_3^{2+}$. While apparent k_q values differed for enantiomeric and racemic $Ru(bpy)_3^{2+}$, both values were large enough with Δ,Λ-$Co(phen)_3^{2+}$ to suggest that the quenching mechanism does not involve actual molecular diffusion of chelate ions over extended distances.[43] As noted already, polarized emission studies had indicated that the rotation of $Ru(bpy)_3^{2+}$ is restricted in the adsorbed state.[15] Consequently, it is likely that such chelates also have low diffusional mobility on clay—i.e., diffusion coefficients much less than the typical value (ca. 5×10^{-6} cm^2 s^{-1}) in water. Such a conclusion also appears to be borne out by the quasi-elastic neutron-scattering studies on hydrated metal ions in clay.[44]

Among other factors, quenching efficiency in clay is probably dictated by proximity effects (static quenching). Such proximity might be ensured by "pseudoracemic" interactions and similarities in the size and charge of the chelate ions. Thus the differences in relative quenching efficiencies in water and in clay might reflect differences in the degree of "integration" of $Ru(bpy)_3^{2+}$ and $M(phen)_3^{n+}$ in the latter. Although a highly efficient quencher in solution, methylviologen (MV^{2+}), for example, fails to quench the excited state of $Ru(bpy)_3^{2+}$ in clay as a result of segregation.[10a,45] The importance of "pseudoracemic" interactions in promoting integration is highlighted by the differences in MLCT λ_{max} (Table V) and excited-state quenching efficiencies (Table IV) between Δ-$(-)_D$- and Λ-$(+)_D$-$Ru(bpy)_3^{2+}$ when Λ-$(+)_D$-Ni-$(phen)_3^{2+}$ and Λ-$(+)_D$-$Rh(phen)_3^{3+}$ are employed as quenchers.[46] Indeed, the absorption spectrum of Λ-$(+)_D$-$Ru(bpy)_3^{2+}$ is unaffected by the presence of the above quenchers, while its excited state is hardly quenched at all!

The perturbing effect of "pseudoracemic" interactions on binding state might also account for the apparent differences in k_q between enantiomeric and racemic forms of $Ru(bpy)_3^{2+*}$. Consider the case of $Co(phen)_3^{2+}$ and $Ni(phen)_3^{2+}$: Apart from differences in the energies of metal-localized orbitals, these chelates are similar to $Zn(phen)_3^{2+}$. The latter has been shown to enhance the emission intensity of enantiomeric $Ru(bpy)_3^{2+*}$ in Na–hectorite

while leaving that of the racemate relatively unperturbed (Figure 9). As suggested already, such modulations in intensity are possibly induced by "pseudoracemic" interactions via π–π overlap. The apparently lower value of k_q for the enantiomers (Table IV) might then be explained in terms of two opposing effects: luminescence enhancement due to "pseudoracemic" interactions and luminescence attenuation due to energy-transfer quenching. While it is tempting to propose that a similar explanation might hold for $Rh(phen)_3^{3+}$ and $Co(phen)_3^{3+}$, preliminary time-resolved emission studies on Δ-$(-)_D$- and Δ,Λ-$Ru(bpy)_3^{2+*}$, in the absence and presence of a stoichiometric equivalent of Λ-$(+)_D$-Rh-$(phen)_3^{3+}$, suggest otherwise: Apart from an attenuation in the signal intensity at time $t = 0$, the emission decay profile of Δ-$(-)_D$-$Ru(bpy)_3^{2+*}$ does not change in the presence of Λ-$(+)_D$-Rh(III). On the other hand, in addition to signal attenuation at $t = 0$, the decay profile of Δ,Λ-$Ru(bpy)_3^{2+*}$ changes in presence of Rh(III), approaching that of Δ-$(-)_D$-$Ru(bpy)_3^{2+*}$. The signal attenuation at $t = 0$ may be ascribed to static quenching by oxidative electron transfer while shape changes are indicative of binding-state perturbation. Presumably unlike in the case of $Zn(phen)_3^{2+}$, "pseudoracemic" interactions with $Rh(phen)_3^{3+}$ lower the emission intensity of Δ,Λ-$Ru(bpy)_3^{2+*}$ while leaving that of the enantiomer relatively unchanged.

Conclusion

From the above results and discussion, it may be concluded that layered clays, both expandable and nonexpandable, promote recognition between optical antipodes of cationic poly(pyridyl) metal complexes. Such chiral interactions—which are partly responsible for the spectral shifts of the racemic complexes upon adsorption—occur spontaneously ($\Delta E \sim -1$ kcal/mol) on clay and are *not* a consequence of steric constraints imposed on the system at high packing densities. Spontaneous chiral interactions, which presumably occur via π–π overlap of partially oriented chelates, also account for many of the intriguing absorption and emission spectral results of $Ru(bpy)_3^{2+}$ in the presence of $M(phen)_3^{n+}$ coadsorbates. We speculate that such interactions might also serve as the driving force for optical resolution of organic racemates whose separation is otherwise difficult to rationalize in terms of the steric model proposed by Yamagishi.[3,47]

(42) Presumably such effects have gone unobserved due to the greater facility of "trivial" quenching at the higher concentrations of $Ni(phen)_3^{2+}$ required for experiments in solution. The concentrating effect of the clays, together with the ability of the chelate to "integrate" with $Ru(bpy)_3^{2+}$ when "pseudoracemic" interaction is possible, obviates the above difficulty and permits "nontrivial" quenching processes to be studied at much lower (ca. 10^3 times) quencher concentrations.

(43) Such a conclusion is also apparent from the self-quenching data on $Ru(bpy)_3^{2+*}$ at high excitation intensity (see ref 39 in ref 10a of this paper).

(44) Tuck, J. J.; Hall, P. L.; Hayes, H. B.; Ross, D. K.; Hayter, J. B. *J. Chem. Soc., Faraday Trans. 1* **1985**, *81*, 833.

(45) $k_q(MV^{2+}) \sim 7.5 \times 10^6$ M^{-1} s^{-1} in clay vs 2.4×10^9 M^{-1} s^{-1} in water (Joshi, V.; Kotkar, D.; Ghosh, P. K. *Curr. Sci.* **1988**, *57*, 567).

(46) There are very few examples of stereoselective reactions between complexes of similar charge. See: Lappin, A. G.; Mortone, D. P.; Osvath, P.; Marasuk, R. A. *Inorg. Chem.* **1988**, *27*, 1863.

(47) Preliminary studies indicate that ($\pm$)-gossypol—a male antiferility agent—may be partially resolved on chirally modified clay columns (Joshi, V.; Ghosh, P. K., unpublished observations).